

A Theory for Migration, Inversion, and Data Mapping Based on the Kirchhoff Approximation

N. Bleistein & J. Stockwell
Center for Wave Phenomena
Colorado School of Mines
Golden, CO 80401-1887

Abstract The Kirchhoff approximation for upward reflection of data is used as a point of departure for the development of a high frequency inversion formalism for imaging reflectors in the earth and estimating parameter changes across those reflectors. Initially, the Kirchhoff representation is given by an integral over a single reflecting surface. A crucial element of this derivation of the inversion formula is the transformation of the Kirchhoff representation of the wave field into a *volume integral* through the use of the *singular function of the surface*, which is a Dirac delta function of a single variable that measures distance from the reflecting surface. Then, we rely on linearity to use the same formula to invert a complete data set in order to obtain a full image of the earth's interior.

The inversion operator also has the structure of a Kirchhoff integral, but now, over the acquisition surface and time or frequency; hence, the name, *Kirchhoff inversion*. Such operators “propagate” the data into the interior of the medium with respect to a “slowly varying” background wave speed. This wave speed is assumed known, although we also allude to methods for its determination through exploitation of the redundancy of data for imaging purposes alone.

The output is an ensemble of singular functions of the reflecting surfaces, each scaled (pointwise) by a specular reflection coefficient, with specular angle arising from the particular source/receiver pair for which the geometrical optics rays satisfy Snell's law at the reflection point. We describe a straightforward method for determining that specular angle.

The method, as presented here, ignores multiple reflections, treating all data as if it arises from primary reflections, only. It also neglects *multi-pathing*—multiple ray trajectories from a single point at depth to a single point on the data acquisition surface.

In summary, the method uses the slowly varying, or low wavenumber part, of the wave speed and (perhaps) other medium parameters to determine the high wave number, or *most singular part*, of the wave speed.

The method is also extended to *Kirchhoff data mapping*. This is a technique for transforming data acquired with one data acquisition geometry and background earth model into another data acquisition geometry and (possibly) different background earth model. Uses of Kirchhoff data mapping are presented in the text. This is a generalization of a technique for transforming data from common (fixed) nonzero offset between source and receiver to zero offset data.

INTRODUCTION

Research in high frequency inverse methods applied to seismic exploration has been conducted for more than twenty years in a coordinated program by the authors and their colleagues. This program started at the University of Denver and then, later and primarily, continued at the Center for Wave Phenomena at the Colorado School of Mines. As an asymptotic theory, the primary focus has been on imaging reflectors and estimating the change in medium parameters across them. The latter is achieved through estimates of the geometrical optics reflection coefficient at one or more specular reflection angles, requiring a further unraveling to actually estimate the medium parameters, themselves.

The methods we use provide a bridge between the classical migration techniques of seismic exploration—originally designed to produce an image of reflectors, only—and the more mathematically sophisticated high frequency techniques based on the generalized Radon transform. Our primary mathematical methods are asymptotics—ray theory or geometrical optics—multi-dimensional stationary phase, and integral transform techniques. Implementation of the methods entails intensive computation. However, the computation has been achievable for two dimensional (2D) earth models for many years and has more recently become tractable for 3D earth models, as well.

The data gathering experiments assumed here are ones in which a source is set off with receivers laid out in a linear, multi-linear or full areal array over an acquisition surface that is not necessarily flat. The entire experiment is then moved and repeated, *many times*. The ensemble of experiments produces redundant data that can provide many images of the same region of the earth. When the receiver array is large enough, data from a single experiment can be used to create an adequate subsurface image (common shot migration or inversion). Alternatively, the data can be re-ordered, say, with fixed separation between source and receiver. Then, one depends on the multiplicity of experiments to provide adequate data coverage to create an image (common offset migration or inversion).

The discussion, here, is totally in the context of the scalar wave equation with constant density. Generalizations appear elsewhere and will be apparent to the sophisticated reader. This simple case is enough to explain the basic ideas of the methodology and, hopefully, will encourage the reader to seek out more complete and more sophisticated expositions.

Furthermore, this theory assumes that we can separate out the primary reflec-

tions from multiples. To the extent that this is not done, multiply reflected energy is processed to generate “ghost” images of the true reflectors. So-called “adaptive deconvolution” methods have been used for multiple elimination in simple earth models; more recently, there have been more ingenious methods proposed for far more general multiple elimination. See Berkhout and Verschuur [1997], Dragoset and MacKay [1993], Ikelle, et al. [1998], Jakubowicz [1998], Weglein, et al. [1998].

This technology transfers to other areas of application where reflector maps and estimation of medium parameters in optically opaque media are an objective. These include other earth applications, such as near surface imaging for a variety of objectives: buried toxic materials, archeological detection, land mine and seamine detection, environmental impact, to name just a few. Note that these involve imaging on a different scale, but high frequency imaging, nonetheless. At a more extreme scale, the methods are applicable to nondestructive evaluation of materials—the detection of flaws and inclusions in solids for the purpose of analyzing material integrity under load. Medical imaging and satellite imaging are two other application areas with extremely different length and time scales.

High frequency

For all of these examples, the high frequency assumption is fundamental. Simply stated, this is the requirement that

$$\lambda = \frac{4\pi f L}{c} \geq \pi. \quad (1)$$

In this equation, f represents a typical frequency in Hz, L is a typical length scale, and c is the wave speed. It is certainly true that high frequency asymptotic theory provides a prediction of accuracy of an approximation in the limit $\lambda \rightarrow \infty$. However, we need a pragmatic criterion that tells us when λ is “large enough.” The one proposed here comes from a comment by J. B. Keller in a math methods class that the first author took in 1962(!): “Three is as close to infinity as one-third is to zero!” It is a matter of practical experience that when $\lambda = 3$, asymptotic expansions of oscillatory functions that are valid as $\lambda \rightarrow \infty$ yield qualitatively accurate and, often, quantitatively “accurate enough” approximate solutions. The use of π instead of 3 on the right side of (1) certainly makes the arithmetic a little easier. Also, with this choice, the constraint is consistent with the Rayleigh criterion in optics, namely that for resolution (defined as the ability to distinguish individual responses to nearby interfaces) at a given frequency, a length scale L is considered large compared to the wavelength, Λ , if

$$L \geq \frac{\Lambda}{4}. \quad (2)$$

For example, for a frequency of 40 Hz in a region with a wave speed of 4000 m/sec, high frequency methods would provide a good approximation of reality if $L \geq 50$ m. This means that the length scales of the problem—the range to the reflector, the radii

of curvature of the reflector, the separation between reflectors, to name just a few length scales, should all be at least 50 m. These are not unreasonable parameters for seismic exploration. On the other hand, for a frequency of 40 KHz and a wave speed of 1500 m/sec, $L \geq 3.75$ cm, not unreasonable for the radius of curvature of a seamine. As a third example, consider a frequency of 4 μ Hz and a wave speed of 6000 m/sec. In this case, $L \geq 1.5$ mm, a realistic length scale for nondestructive testing in titanium. In practice, it is the length scales and wave speed that dictate the frequency of the experiment. All we have shown here are self-consistent sets of parameters for high frequency inversion to be a practical choice.

There is one modification of this criterion that becomes important when the sources and receivers are separated. In that case, (1) should be replaced by

$$\lambda = \frac{4\pi f L \cos \theta}{c} \geq \pi. \quad (3)$$

Here, θ is half the opening angle between rays from the specular source and receiver points where they meet at the image point. The effect of separating the source and receiver is to scale the aperture in the wave-vector domain by this factor of $\cos \theta$, and this, in turn, leads to a loss of resolution in the spatial domain where the width of the main lobe of bandlimited delta functions delineating reflectors is broadened by $\sec \theta$.

Inversion on a shoestring

As a prelude, we present a simple acoustical example here to introduce the reader to the basic ideas of the method. Figure 1 shows an earth model with a single reflecting surface in 2D. Above the model is a display of data traces that would be produced at 81 locations above the reflector, assuming a coincident source and receiver. The source, itself, was a bandlimited pulse. The wave speed used for this synthetically generated data was 2 km/sec. Thus, the geometrical optics rays are straight lines. The primary returns—specular reflections—occur at those points where the ray from source/receiver point is normal to the reflector. At these points, the incident and reflected rays make equal angles (zero) with the normal to the reflector.

The display of traces requires some explanation. Each trace number corresponds to a physical location on the upper surface. The vertical axis is time in seconds. We need a *third* coordinate to measure amplitude of the “impulse response” of the earth. That has been resolved here by laying the data trace back down into the plane with positive amplitude represented as deviation to the right of the vertical line directly below the trace location and negative amplitude representing deviation to the left of the vertical line. Thus, for the trace at the far left, all of the “action”—the nonzero values—are centered around one second. This is the two-way travel time for a pulse to propagate down to the horizontal portion of the reflector, reflect normally, and return to the coincident receiver. Only a few traces over, however, we see two returns on the trace and, further on, three returns. It is left as an exercise for the reader to find the additional specular points on the reflector; that is, find the points on the

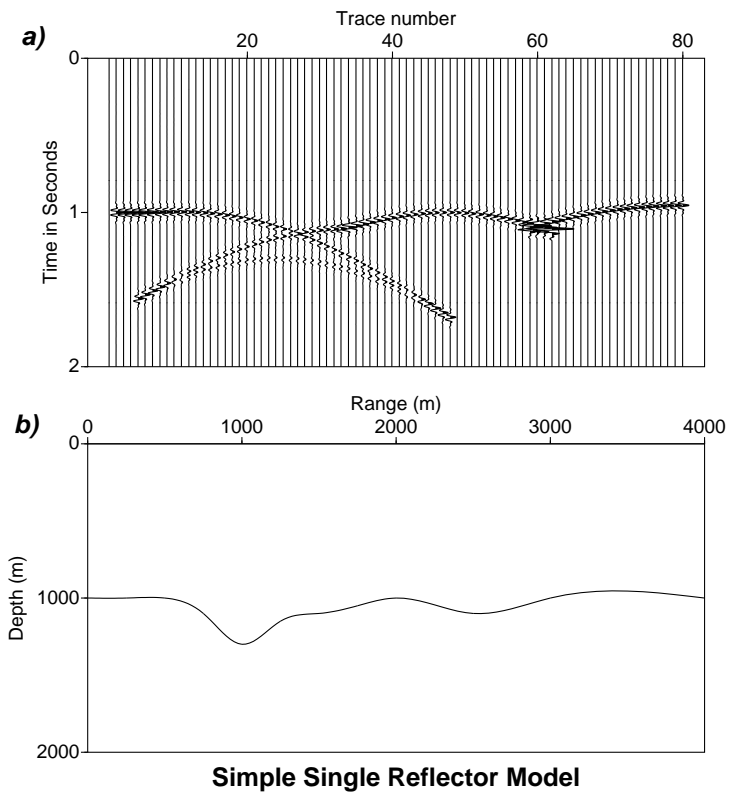


FIG. 1. a) A synthetic *zero-offset* seismic section and b) earth model. The synthetic was made with the program *cshot*.

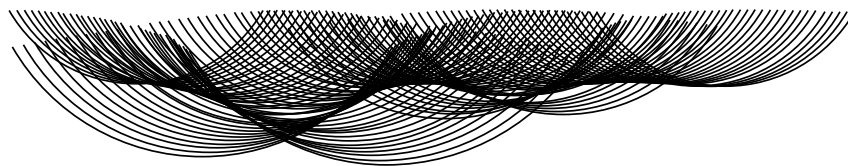


FIG. 2. An example of graphical migration. Plot done by Herman Jaramillo and Andreas Rueger when they took the inversion course at CWP.

reflector for which the ray from the coincident source/receiver is normal there. The relative lengths of those lines predicts the location of the relative arrivals on the trace. In fact, for the length scales that were used to depict time in Part *a* and depth in Part *b*, a compass could be used to “migrate” the reflection point in Part *b* to the arrival time on a trace in Part *a*. On a larger plot, say on a blackboard, a shoestring, with a piece of chalk attached, works very well as a compass, so this is modeling on a shoestring—low cost computing, to be sure!

Reversing the process is somewhat harder. Given a reflection “event” on a trace in Part *a*, all one can be sure of, is that it came from somewhere on a circle in the physical domain in Part *b*, having a radius equal to the one way travel distance consistent with the wave speed and travel time of the event in Part *a*. However, if one draws all of those circles, then the *envelope* of the family of circles is a curve for which every point satisfies the appropriate specular reflection condition and produces a reflection event at precisely the right position in Part *a*. See Figure 2. Here, we have taken the data in time domain and graphically moved it—migrated it—back to its spatial position by looking at all possible candidate positions and then choosing the envelope as the coherent reflector image. A compass will do this construction on paper, but, again, a shoestring works fine on a blackboard-sized image of the data. This graphical technique [Haagedorn, 1954] precedes and anticipates more sophisticated methods of producing reflector maps and was the method of choice before computer processing of data was available.

A mathematical insight

Let us look, now, at the mathematical process of generating the envelope of a family of curves. In doing so, we will use a notation that anticipates the discussions of later sections. We denote by ξ , the x -coordinate of the trace location, and we denote by $t(\xi)$, the observed travel time of the peak on the trace. We think of the peak time as being “zero-time” for the source wavelet that propagated downward and was ultimately reflected back to the coincident receiver. Then the peak time of the return represents the two-way travel time of the reflection response. From that response, we could only say that there was a reflection somewhere on an equi-travel-time curve, an *isochron*, in \mathbf{x} . This equation has the form

$$t(\xi) - \tau(\mathbf{x}, \mathbf{x}_s(\xi), \mathbf{x}_g(\xi)) = 0. \quad (4)$$

Here, τ represents the travel time from the source, to the “scattering point” at depth, to the receiver (geophone, hence subscript, g).

We are being somewhat elaborate to describe this simple situation in which the source and receiver are coincident and have coordinates,

$$\mathbf{x}_s(\xi) = \mathbf{x}_g(\xi) = (\xi, 0), \quad (5)$$

with the travel time curves simply being circles with radius is $ct(\xi)/2$ and center, $(\xi, 0)$. However, we are suggesting a more general application of this simple idea by our notation. The source and receiver could be separated, the travel time could be a sum of solutions to the eikonal equation and *mathematically* we could still contemplate determining the reflector by seeking out the envelope of the family of travel time curves with respect to the parameter, ξ , just as we did in the shoestring construction, above.

Recall that to find the envelope of this family of curves, we set the first derivative of the left side in (4) equal to zero, solve for ξ as a function of \mathbf{x} , and substituting back into (4). There is another process in which we find a “critical value” of a parameter by setting the first derivative of a function equal to zero and then substitute back into the original function. That process is the *method of stationary phase*. Below, we will generate inversion operators with a phase function of the form, $-i\omega\tau(\mathbf{x}, \mathbf{x}_s(\xi), \mathbf{x}_g(\xi))$. Inversion will require integration in ξ (which amounts to summation over source/receiver pairs) and then integration over ω (which, the migrationists will tell you, amounts to sending the signal from $z = 0$ at all time, back to the depth of its origination at $t = 0$ at half the wave speed). When testing this operator on ray data or Kirchhoff-approximate data, we will find that the data includes a phase factor of the form, $i\omega t(\xi)$, with $t(\xi)$ being the model travel time on the specular ray path from the source to the reflector to the receiver. Thus, we will be considering integrals of the form,

$$\beta(\mathbf{x}) = \int G(\omega, \xi, \mathbf{x}) e^{i\omega\phi(\mathbf{x}, \mathbf{x}_s(\xi), \mathbf{x}_g(\xi))} d\omega d\xi, \quad (6)$$

with

$$\phi(\mathbf{x}, \mathbf{x}_s(\xi), \mathbf{x}_g(\xi)) = t(\xi) - \tau(\mathbf{x}, \mathbf{x}_s(\xi), \mathbf{x}_g(\xi)), \quad (7)$$

and G just representing all of the amplitude of the integrand resulting from the application of the operator to model data.

To approximate the ξ -integration by the method of stationary phase, we would

- i** set the first derivative of ϕ with respect to ξ equal to zero;
- ii** use that equation to solve for ξ as a function of \mathbf{x} ;
- iii** substitute that value back into ϕ and G and apply the appropriate formula to obtain the stationary phase approximation to that integral.

Note that {i} and {ii} are the same steps that we take in defining an envelope. However, here, there is no *a priori* reason to set $\phi = 0$. Instead, let us think of setting $\phi = \text{constant}$ for a moment. For each choice of that constant, letting ξ vary generates a family of curves in the \mathbf{x} -domain. Then, we can think of the stationary value of ξ as determining the envelope of the family of curves for each constant value of ϕ . Again, the value $\phi = 0$ is special, because it is the actual reflector, but it has not as yet been distinguished in the stationary phase process. However, after the application of stationary phase, it will turn out that the resulting integrand has the form,

$$\beta(\mathbf{x}) = H(\mathbf{x}) \int F(\omega) e^{i\omega\phi} d\omega, \quad (8)$$

with H a “slowly” varying function over the wavelengths consistent with the support of $F(\omega)$ and this latter function being the original source signature in the frequency domain.

In this theory, the sources are assumed to be impulses—bandlimited delta functions—that peak at argument zero. Thus, within a scale factor,

$$\beta(\mathbf{x}) \sim \delta_B(\phi). \quad (9)$$

Here, $\delta(\phi)$ is the Dirac delta function of argument ϕ ; hence, its support is on the reflector, where $\phi = 0$. The subscript B connotes *bandlimited*, due to the finite extent in the frequency domain of the source signature (and further attenuation in the real problem being modeled here). The theory, then, will predict that if we apply an operator with this travel time phase to bandlimited impulse response data as appears in Figure 1, the result will be a bandlimited delta function of an argument that is zero on the reflector. (From the fact that the \mathbf{x} -gradient of the travel time is nonzero, we can even show that this function is not zero elsewhere in a neighborhood of the reflector.)

Consequently, the theory is the means by which we turn the shoestring construction into a viable mathematical method which relates the amplitude of the output to the reflection coefficient and becomes a point of departure for generalizations to more accurate physical models and to situations in which simple ray theory breaks down.

Inversion and velocity analysis

Note that, in order to find our simple reflector, we needed to know the wave speed above the reflector. For an incorrect wave speed, we would have determined the envelopes of a family of circles, all of which had the wrong radius. That would have led to the wrong image. In practice then, it is necessary to have some means of estimating that wave speed above a reflector before imaging it. Fortunately, experimental practice provides redundant images of reflectors. The extent to which they do not line up is an indicator of the inaccuracy of the wave speed and provides a means of correcting that wave speed. Many ingenious methods have been developed in recent years to do just this in progressively more complicated earth models. Thus,